Experimental investigations on the fatigue resistance of automatically welded tubular X-joints for jacket support structures

Experimental investigations on the fatigue resistance of automatically welded tubular X-joints for jacket support structures

K Schürmann[1], P Schaumann[1], A Pittner[2] and M Rethmeier[3,2]

[1] Leibniz University Hannover, Institute for Steel Construction – ForWind Hannover, Appelstraße 9A, 30167 Hanover, Germany
[2] Federal Institute for Materials Research and Testing (BAM), Unter den Eichen 87, 12205 Berlin, Germany
[3] Technical University of Berlin, Institute of Machine Tools and Factory Management, Pascalstr. 8-9, 10587 Berlin, Germany

schuermann@stahl.uni-hannover.de

Abstract. The development within the offshore wind sector towards more powerful turbines combined with increasing water depth for new wind parks is challenging both the designer as well as the manufacturer of bottom fixed support structures. Besides XL-monopiles, the market developed an innovative and economic jacket support structure which is based on automatically manufactured tubular joints combined with standardized pipes. Besides the improvements for a serial manufacturing process the automatically welded tubular joints show a great potential in terms of fatigue resistance e.g. due to a smooth weld geometry without sharp notches. However, these benefits are not considered yet within the fatigue design process of automatically manufactured jacket substructures according to current standards due to the lack of suitable S-N curves. Therefore, 32 axial fatigue tests on single and double-sided automatically welded tubular X-joints have been performed to determine a new hot spot stress related S-N curve. Based on these constant amplitude fatigue tests a new S-N curve equal to a FAT 126 curve was computed which implicitly includes the benefits of the automatically welding procedure.

1. Introduction

Based on the German strategy of planning offshore wind farms as far away from the coastline as possible, most of the wind farms in Germany's Exclusive Economic Zone have water depths of around 35 m and more. In addition to (XL-) monopiles, lattice support structures such as jackets can be considered as foundation structure for these water depths, see Figure 1. For example, in the Baltic Sea 41 jackets with water depths greater than 35 m were installed in the wind farm Baltic II. Furthermore, 70 wind turbines of the 5 MW class were installed on jackets at a water depth of 37 - 43 m in the Viking wind farm located in the Baltic Sea as well.

Jacket foundation structures are designed as spatial tubular hollow section steel structures based on the construction of oil and gas platforms and are characterized by high rigidity with low material consumption [1]. The spatial structure of the jacket is created with the typical tubular connection variants double-K-, X- and double-Y-joints.

Figure 1. Offshore wind energy turbine with jacket support structure from the offshore wind farm alpha ventus

Especially for jackets, the optimization potential for production and design is almost unused. An essential component of this optimization is the individual production of the tubular joints combined with the use of standardized pipes. This modular principle enables an automatic production of the tubular joints, which increases the competitiveness of the jackets especially against the background of the large quantities required for offshore wind farms [2].

Besides the improvements for a serial manufacturing process, the automatically welded tubular joints show a great potential in terms of fatigue resistance e.g. due to a smooth weld geometry without sharp notches. However, these benefits are not considered yet within the fatigue design process of automatically manufactured jacket substructures according to standards and guidelines due to the lack of suitable S-N curves.

Therefore, this contribution presents new S-N curves for automatically welded tubular X-joints which were determined within the joint FOSTA research project (AiF) "FATInWeld" of the Institute for Steel Construction at Leibniz University Hannover and the Federal Institute for Materials Research and Testing (BAM).

2. Automated gas metal arc welding procedure for tubular joints

The automated manufacturing of tubular joints for offshore jacket substructures not only reduces production costs but also enables a transition from a point-to-point production to a manufacturing segmentation, based on automatically manufactured tubular joints combined with standardized pipes. The automatically welding procedure of tubular joints was therefore applied on scaled tubular X-joints which had a scaling of 1 : 3.3 compared to real dimensioned tubular joints of offshore jacket substructures. The considered X-joint was designed for test purposes and meets the dimensionless parameter according to Figure 2 considering a diameter of the chord of D = 368.0 mm and a chord-brace angle $\Theta = 60°$.

The design of the HV seam preparation along the three-dimensional intersection geometry of the X-joint was CAD-supported. Care was taken to ensure that the cross-sectional areas in the range 45°-315° in direction of rotation (Figure 3) were constant with a seam opening angle of 45°. In the 315°-45° range, the seam opening angle was continuously reduced to a minimum of 30° (position 0°).

Since deviations in diameter and wall thickness from the nominal values of the standard tubes lead to significant local deviations in the weld preparation, the geometric tolerances of the chord and brace tubes are of high relevance. In order to minimize the deviations within the weld preparation, the tolerances of the tubes were recorded and individual CAD data was used for the manufacturing of the weld preparation. The seam preparation of the brace stub was then manufactured by milling.

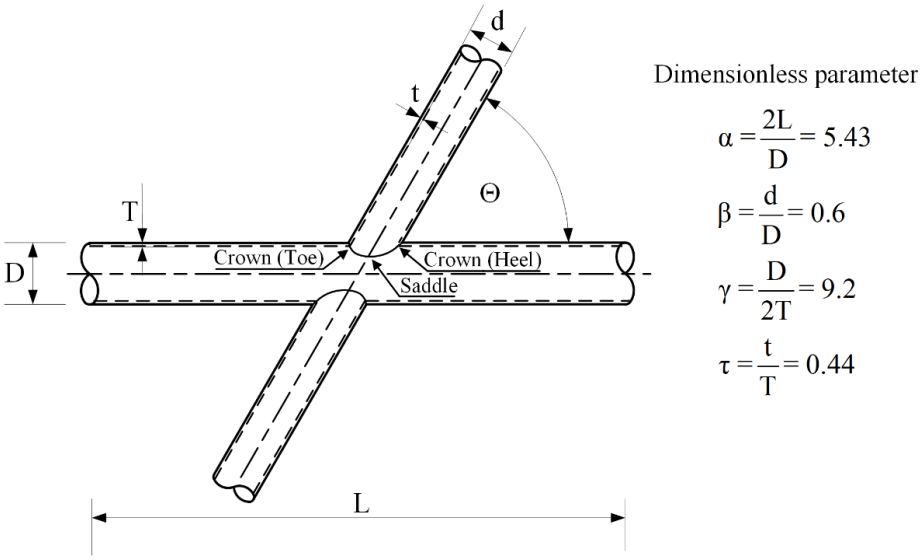

Figure 2. Geometry definition of tubular X-joint according to [3]

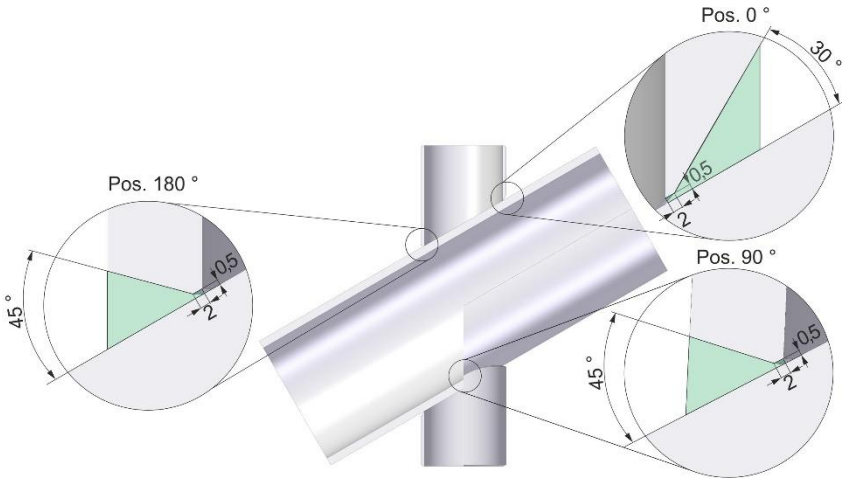

Figure 3. Weld seam preparation for the automated welding of the tubular X-joints according to [4]

The welding process was designed on the basis of the seam preparation defined in Figure 3. With regard to the material specifications the brace stubs were made of S355J2H according to EN 10210-1 [5]. The chord tubes were made of S355J2H with the additional quality Z35. A solid wire with a diameter of 1.2 mm of quality G 46 6 M21 3Ni1 according to EN ISO 14341 [6] was used as filler material. As shown in Figure 4, left, the welding process started at -45° (or 315°) with a linearly increased wire feed rate from 7.5 m/min to 11.5 m/min. The process parameters remained constant in the 45°-315° range. From the 315° position, the wire feed rate was reduced linearly to 8.5 m/min at 45° (or 405°). During the welding process each X-joint got its own work piece identification number (WiD) to enable a full traceability of the recorded data sets. Related to the welded tubular X-joint, the 0° position corresponds to the crown heel, the 90° position belongs to the saddle and the 180° position corresponds to the crown toe.

More detailed information about the welding procedure as well as the performed data acquisition and storage along the welding process chain including laser scanning of the weld seam geometry are given in [4] and [7].

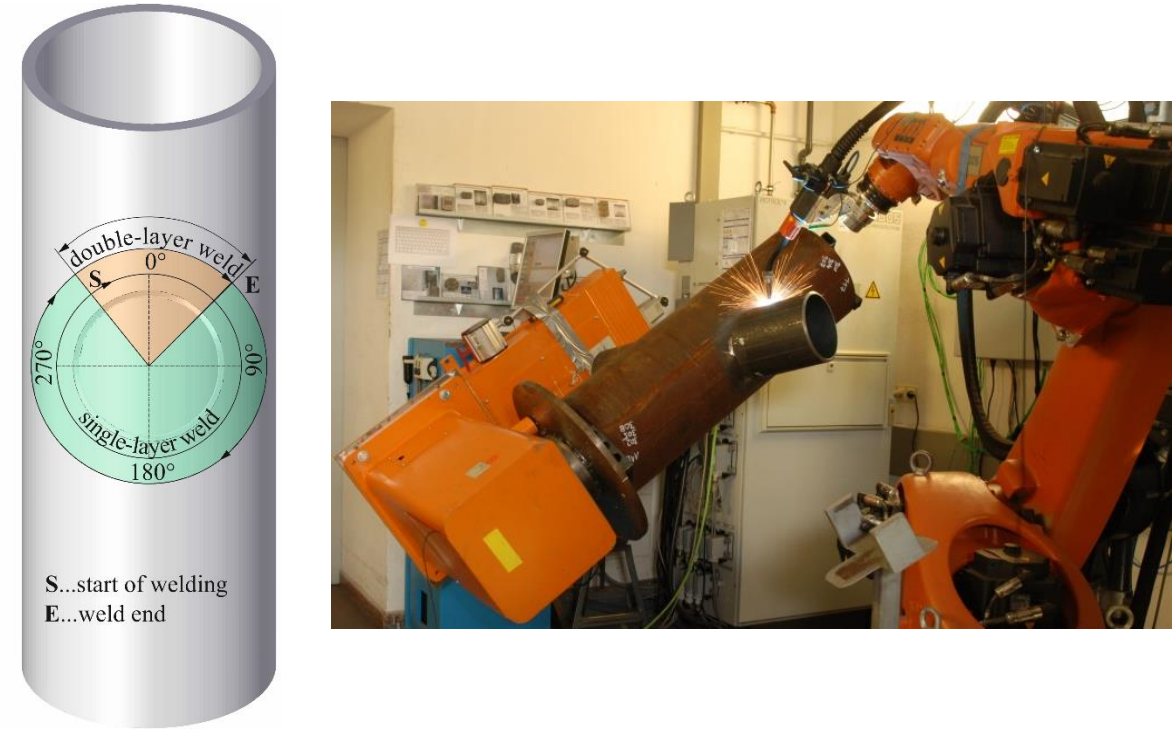

Figure 4. Left: Setup of the gas metal arc welding process along the weld trajectory according to [4]; Right: Automated gas metal arc welding procedure of a tubular X-joint

3. Axial fatigue tests on automatically welded tubular X-joints

3.1. Failure criterion

For fatigue tests of tubular joints the through thickness crack is a well-established failure criterion due to its objective detection opportunity by observing a loss of over or under pressure within the pipes of the failed tubular joint [8], [9]. Additionally, this failure mode is predicted by the structural stress approach, which is the state of the art for the fatigue design of tubular joints [3]. Therefore, the through thickness crack was decisive for the performed fatigue tests of the automatically welded tubular X-joints. Referring to [8], the corresponding number of load cycles N for through thickness cracking is called N_3 in this contribution.

During the fatigue tests the through thickness crack has been observed by detecting a change of inner pressure within the three pipes. Therefore, an over pressure (1 bar) has been applied within the two braces as well as a negative pressure (-0.5 bar) within the chord. During the occurrence of the through thickness crack the inner pressure will equalize with the ambient pressure which is then detected by three absolute pressure transducers. Due to the negative pressure within the chord an inner through thickness crack between brace and chord can be detected as well.

3.2. Test program

The test program to determine a new S-N curve for automatically welded tubular X-joints comprised a total of 32 axial constant amplitude fatigue tests divided into two test series. Both test series (16 tests per series) were identical except of an additional inner root layer within the X-joints for the second series to quantify the effects of this additional inner welding on the fatigue resistant of the tubular joints.

3.3. Test setup and specimen preparation

The fatigue tests have been performed considering a bottom to top load ratio of R = 0.1 and a testing frequency of 5 Hz applying constant amplitude values within a force controlled 1 MN (dynamic) servo

hydraulic testing device. The adaptation of the X-joint to the testing device was realized by a bolted ring flange connection between the X-joint and two adapter plates as shown in Figure 5. Therefore, the automatically welded X-joints were prepared by adding ring flanges on top of the braces followed by planar parallel milling of the ring flange surfaces to guarantee an axial installation within the testing device. Additionally, to ensure identical testing conditions during all fatigue tests, the adapter plates previously installed in the testing device were not removed during the test series.

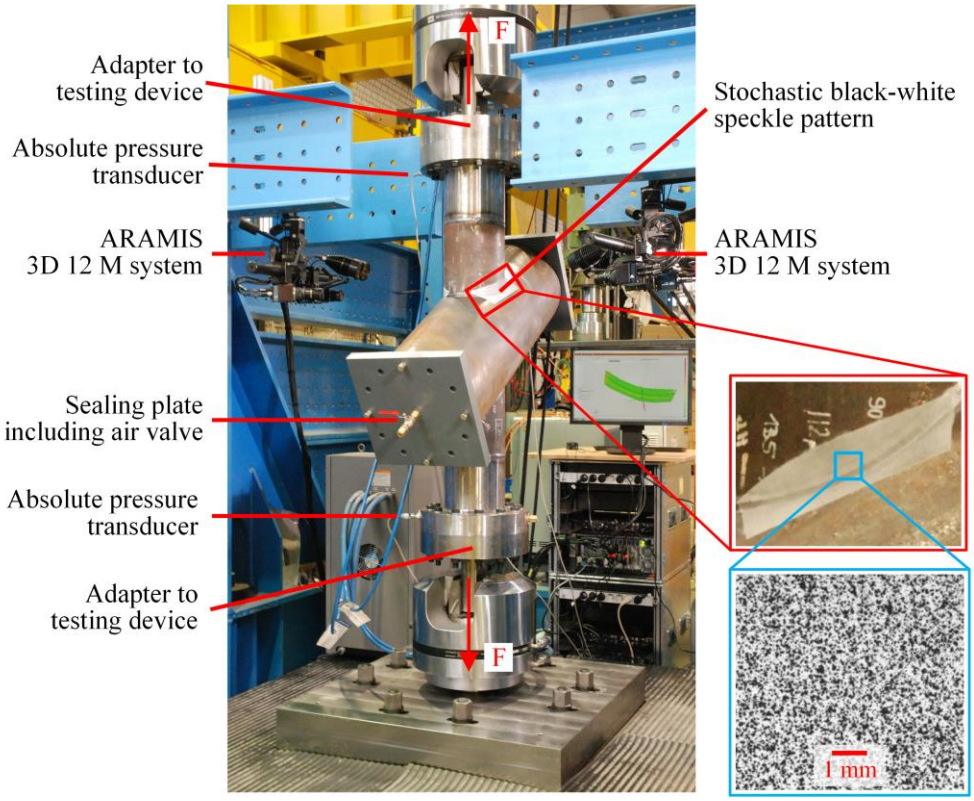

Figure 5. Test setup of the axial fatigue tests

The sealing of the bracings for the detection of the through thickness crack was ensured by an O-ring which was clamped within the ring flange connection. The chord was sealed by two sealing plates including grooves for the chord of the X-joints. The sealing between the sealing plate and the chord was realized by a silicone seal which was previously inserted into the groove. The contact pressure required for the sealing of the chord was ensured by the slightly applied evacuation.

Besides the observation of the inner pressure to detect the through thickness crack, the digital image correlation (DIC) method was applied during 13 fatigue tests per series to digitize the fatigue damage development within the hot spots of the automatically welded tubular X-joints. Therefore, two ARAMIS 3D 12M DIC systems have been utilized. Periodically, at the maximum load a picture of the prepared hot spot was simultaneously taken by both ARAMIS systems. Therefore, the first system (the master system) was triggered directly by the load signal of the testing device. The second ARAMIS system (the slave system) was controlled by the master system by sending a trigger signal at each time a picture was taken. To reduce the required storage space and hence to enlarge the monitorable number of cycles N not every pair of pictures was stored depending on the expected number of cycles.

To ensure a high quality digital image correlation measurement using the ARAMIS systems a high-contrast surface with a unique grey value distribution is essential. Therefore, a stochastic black-white speckle pattern was applied at the upper two hot spot regions of the X-joints indicated by the red box in Figure 5. At a first step the specimen was coated with white powder utilizing the developer known from

the dye penetrant inspection. After drying, black liquid graphite was sprayed on the white surface until a uniform back-white distribution was given. These coating substances were applied instead of corresponding lacquers to allow crack opening of the coating after crack initiation within the specimen.

The tubular X-joints to be tested are double symmetrical test specimens with a total of four possible fatigue critical hot spots. Since only the two hot spots of the upper brace could be monitored with the ARAMIS systems, the fatigue resistance of the two lower hot spots was improved by using the pneumatic impact treatment (PIT) needle peening method. By doing so, the fatigue decisive notch was ensured to be within the monitored hot spots of the upper brace.

4. Fatigue test results

4.1. Fatigue damage behaviour of the automatically welded tubular X-joints

For the presented investigations on the fatigue behaviour of automatically manufactured tubular X-joints, the distribution and propagation of the fatigue induced damage is of great importance, e.g. to improve the welding process with regard to a more fatigue-proof weld geometry or to validate numerical models. To localize these damage hot spots, the local strain distribution ε_x perpendicular to the crack path was computed and visualized by the ARAMIS 2017 software.

Figure 6 exemplarily shows the development of the fatigue induced damage within the considered hot spots located at the saddle position (see Figure 6, a)) for a certain single-sided automatically welded X-joint (WiD 231), which was loaded with a nominal stress range of $\Delta\sigma_N = 41.3$ N/mm². Equivalent results were obtained for the double-sided automatically welded tubular X-joints as well.

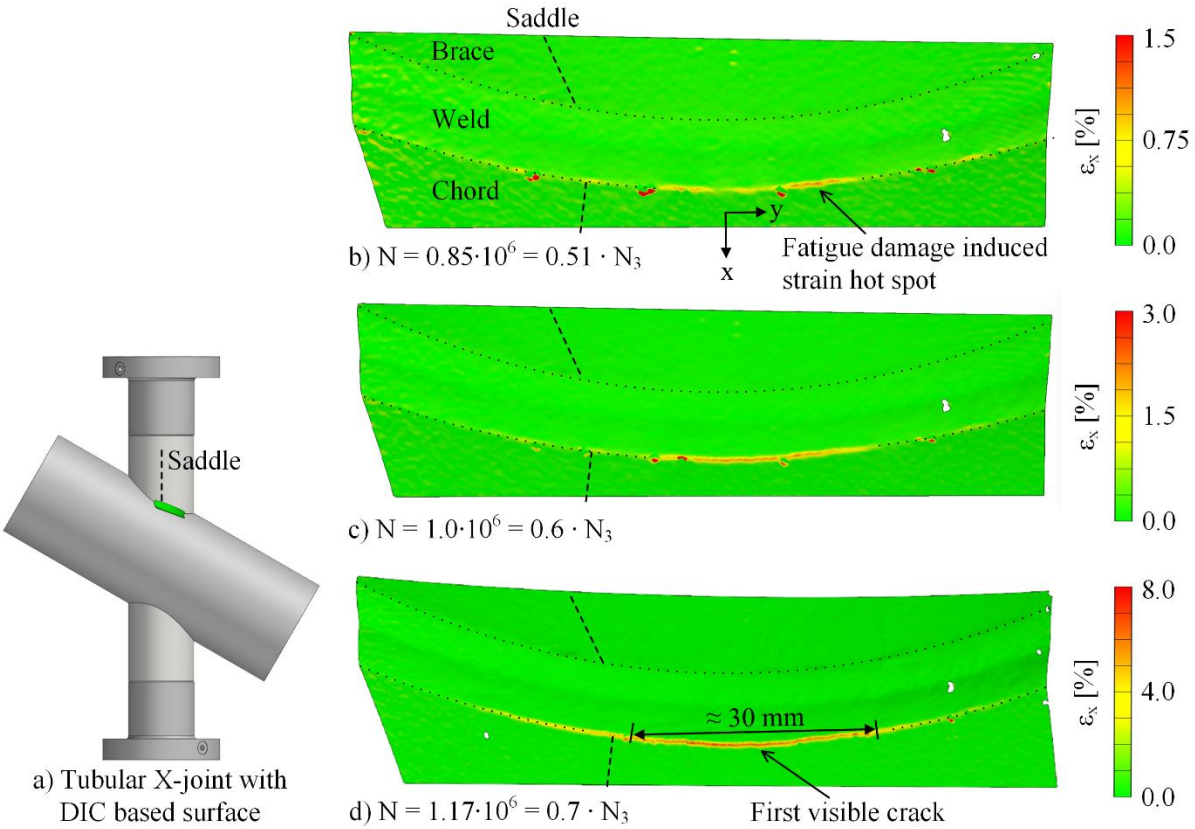

Figure 6. Exemplary fatigue damage behavior within the hot spot of a tubular X-joint

Within Figure 6, b) several damage induced strain hot spots can be seen within the cord-sided notch close to the saddle position. These relatively widely distributed hot spots increased and merged during the ongoing fatigue test so that an increased damaged area was observed within the chord-sided notch after approx. $1.0 \cdot 10^6$ load cycles as shown in Figure 6, c). Additionally, Figure 6, c) shows that the fatigue induced strain ε_x and hence the corresponding damage within the merged hot spot is uniformly distributed without any extreme values. This is due to the typical uniform and smooth weld geometry of the automatically welded tubular X-joints which do not have any locally occurring sharp notches. Finally, a first crack was visually detected in the ARAMIS images (Figure 6, d)) after $1.17 \cdot 10^6$ load cycles, which had a crack length of approximately 30 mm. Comparable crack lengths of the first visually in the ARAMIS images detectable cracks could be confirmed for other tested X-joints independently of the applied load and test series. Attention must be drawn in Figure 6 b)-d) to the fact that no damage was detected within the brace-sided notch.

Figure 7 presents a typical crack path along the chord-sided notch (marked with a white marking pen) after through thickness cracking which is valid for both single and double-sided automatically welded X-joints.

Figure 7. Exemplary crack path after through thickness cracking

Besides the crack propagation along the surface, also the crack path though the chord was similar between both X-joint variants and independent on the considered hot spot position (90° or 270°), see Figure 8. For the tested automatically welded X-joints combined with the applied axial loading the weld root was not fatigue critical and all 32 tested X-joints failed from the outside with crack initiation in the chord-sided notch.

Comparable to the well-known positive effect of the needle peening method on the fatigue resistance of manually welded tubular joints, the outcomes of the performed fatigue tests indicate without quantification that the fatigue resistance of the automatically welded tubular joints can also be improved by applying the needle peening method. None of the tested automatically welded tubular X-joints failed within the lower fatigue improved hot spots.

4.2. S-N curves for automatically welded tubular X-joints

Since the structural stress approach is the state of the art for the fatigue design of tubular joints for jacket support structures, the decisive hot spot stress σ_{HS} and hence the corresponding stress concentration factor (SCF) with SCF = σ_{HS}/σ_N has to be determined to compute the hot spot stress based S-N curve for the automatically welded tubular X-joints.

4.2.1. Numerical determination of decisive SCFs

For the numerical computation of the decisive SCFs a numerical model of both X-joint variants – single and double-sided automatically welded – was generated by using the finite element software ANSYS 17.2. The X-Joints were modelled according to the requirements of the DNVGL-RP-C203 recommendation [3] including the weld geometries, which were based on the profiles obtained from the

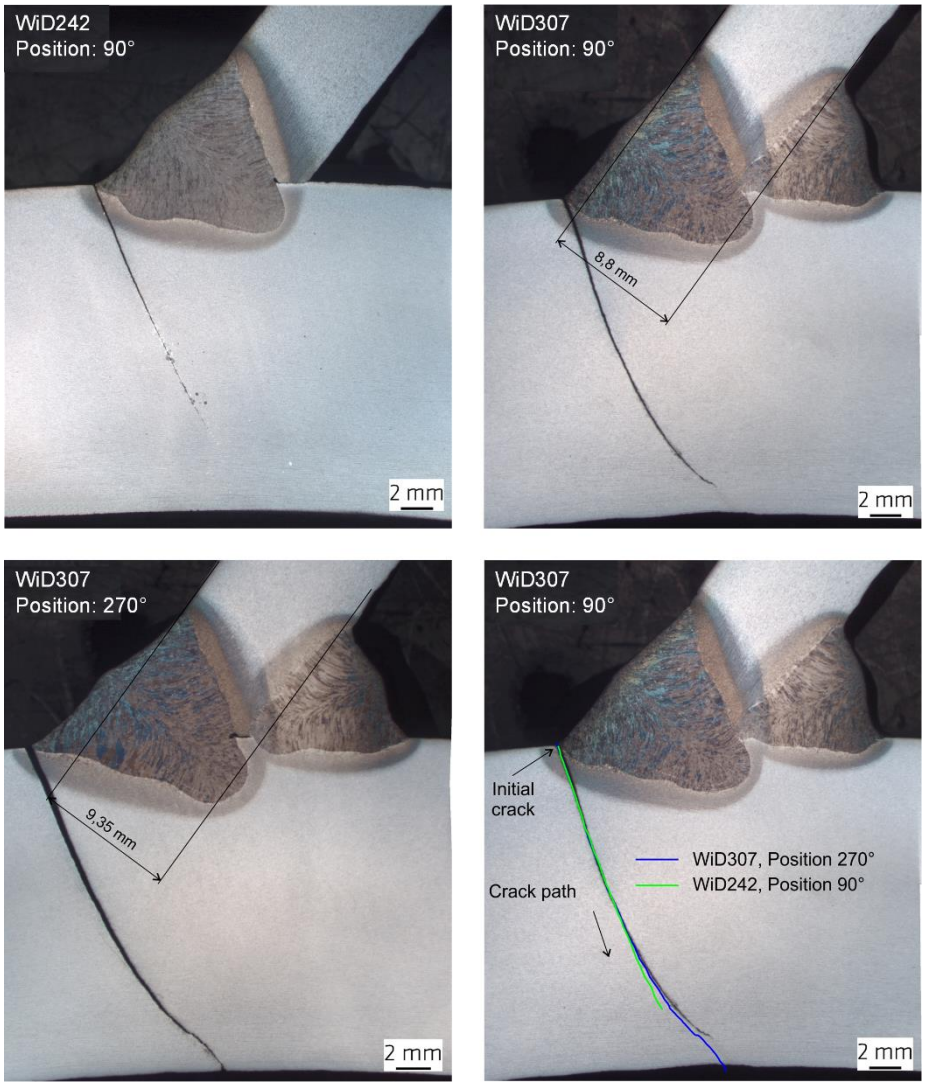

Figure 8. Comparison of crack paths through the cord for both X-joint variants and hot spot positions

laser scanning data. For both numerical models 20-node solid elements (Solid 186) with quadratic shape functions were utilized considering linear elastic material behaviour with a measured Young's modulus of E_{Ch} = 205,667 N/mm² for the chord and E_{Br} = 208,167 N/mm² for the brace. The Poisson's ratio was set to $\nu = 0.3$. Within a sensitivity study the density of the mesh was optimized such that the values of the SCFs were not affected by the mesh. The axial unit load F was applied on top of the upper brace whereas the lower brace was fixed.

The linear extrapolation of σ_{HS} by using the reference points according to DNVGL-RP-C203 [3] was performed on behalf of nine extrapolation paths for the chord and the brace around one half of the chord to brace intersection. Since all performed fatigue tests failed within the chord-sided notch close to the saddle position, the maximum SCF values for the chord were taken for the computation of the S-N curves, see equations (1) and (2).

$$SCF_{Ch,single} = 4.36 \quad (1)$$

$$SCF_{Ch,double} = 4.41 \quad (2)$$

Further detailed information about the numerical modelling of the X-joints and the distribution of the resulting SCF values are given in [10], [4] and [7].

4.2.2. S-N curves for the automatically welded tubular X-joints

The corresponding hot spot stress based S-N curves were determined by further processing the obtained number of load cycles N_3 for through thickness cracking combined with the applied hot spot stress range $\Delta\sigma_{HS}$. The statistical evaluation of the S-N curves were therefore based on the background documentation of the Eurocode 3 [11] fatigue design rules [12]. Figure 9 presents the S-N curves for both the single and double-sided automatically welded X-joints. For the computation of the respective hot spot stress ranges $\Delta\sigma_{HS}$ of both X-joint variants the corresponding SCF values according to equations (1) and (2) were used to include the effect of the inner welding on the applied loading.

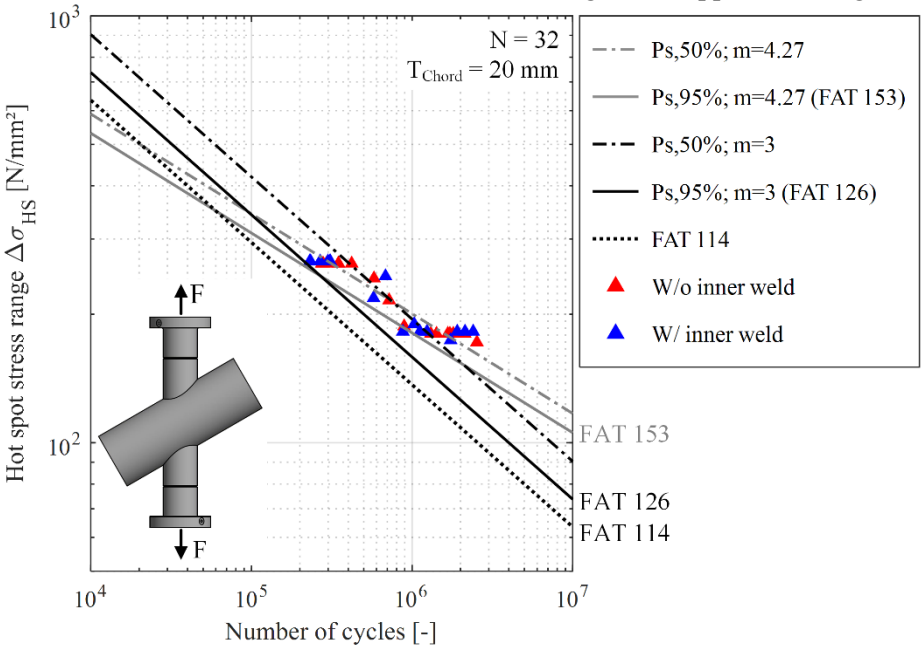

Figure 9. S-N curves for the single and double-sided automatically welded tubular X-joints

For the 32 tested automatically welded tubular X-joints a FAT 126 curve with a fixed slope of m = 3 respectively a FAT 153 curve with a variable slope of m = 4.27 was determined. The current design S-N curve FAT 114 (m = 3) according to DNVGL-RP-C203 is shown in Figure 9 as well. The standard deviation s_N is equal to $s_N = 0.147$ for the FAT 126 curve with m = 3 and $s_N = 0.109$ for the FAT 153 curve with m = 4.27.

5. Discussion of the obtained results

For the performed fatigue tests on the single and double-sided automatically welded tubular X-joints no significant difference between both test series could be determined. Neither the locations of crack initiation nor the resulting crack paths showed any significant differences between the two test series. The obtained scatter bands within the S-N chart are similar for both test series as well. Hence no significant effect of the internal welding on the fatigue resistance and behaviour of the automatically welded tubular X-joints was determined.

For the used test setup with an X-shaped tubular joint combined with an applied axial loading only the outside notches experience tensional stress. The inside notch at the weld root experiences only compressive stresses which causes a stop of crack propagation starting at the weld root. Therefore, the inner root layer does not have a significant effect on the fatigue resistance of the tubular X-joints.

However, the application of an inner root layer improves the safety during automated welding by compensating tolerances of the groove geometry.

6. Summary and outlook

A total of 32 fatigue tests on single and double-sided automatically welded tubular X-joints have been performed. During the fatigue tests two ARAMIS digital image correlation systems were applied to monitor the fatigue damage process within the hot spot of the tubular joints. The outcomes of these optical measurement systems showed a uniformly distributed damage process within the hot spots due to the smooth and uniform shape of the weld geometry without sharp notches. Finally, for the automatically welded tubular X-joints an increased S-N curve equal to a FAT 126 curve with a fixed slope of m = 3 was determined. Considering the variable slope of the test series m = 4.27 an improved S-N curve of FAT 153 was obtained.

The investigated tubular X-joints were medium scaled including a single layer weld compared to realistic offshore jacket tubular joints. Therefore, the fatigue resistance of various shaped and realistic dimensioned automatically welded tubular joints should investigated within future projects.

Acknowledgement

The presented results were developed within the German FOSTA joint research project 'FATInWeld' supported via AiF (IGF 19104 N) within the programme for promoting the Industrial Collective Research (IGF) of the German Ministry of Economic Affairs and Energy (BMWi), based on a resolution of the German Parliament. The authors express their deep gratitude for the financial support received from the BMWi, the AiF, the FOSTA and from the companies involved in the project.

References

[1] Seidel M 2007 Jacket substructures for the REpower 5M wind turbine *Proc. Europ. Offshore Wind Conf. (Berlin)*
[2] Michels G and Brauser S 2014 Salzgitter Supply Chain Concept for Industrial Assembling of Offshore-Wind-Jackets *Proc. Int. Wind Engineering Conf. (Hanover 4 September 2014)*
[3] DNV-RP-C203 2016 *Fatigue Design of Offshore Steel Structures* Det Norske Veritas AS
[4] Schaumann P, Rethmeier M, Schürmann K, Pittner A, Dänekas C and Schippereit C 2018 Automated manufacturing of tubular joints for jacket support structures - description of the welding process chain as well as integration of the process parameters within the fatigue design *Stahlbau* **87** 9 897–909 doi: 10.1002/stab.201810017
[5] EN 10210-1 2016 *Hot finished structural hollow sections of non-alloy and fine grain steels - Part 1: Technical delivery conditions* (Berlin: Beuth)
[6] EN ISO 14341 2011 *Welding consumables - Wire electrodes and weld deposits for gas shielded metal arc welding of non alloy and fine grain steels – Classification* (Berlin: Beuth)
[7] Schaumann P, Schürmann K, Pittner A and Rethmeier M 2019 Automatically Welded Tubular X-Joints - Welding Procedure and Prediction of the Technical Fatigue Crack Location *Proc. 29th Int. Ocean and Polar Engineering Conf. (Honolulu 16–21 June 2019)* 4098–4105
[8] Van Wingerde A M, van Delft D R V, Wardenier J and Packer J A 1997 Scale effects on the fatigue behaviour of tubular structures *Proc. IIW Int. Conf. on Performance of Dynamically Loaded Welded Structures (San Francisco 14 –15 July 1997)*
[9] OTH 92 390 1999 *Background to New Fatigue Guidance for Steel Joints and Connections in Offshore Structures (Health and Safety Executive (HSE))*
[10] Schaumann P and Schürmann K 2019 New proposal to express notch stress approach results by equivalent SCFs *Int. J. Fatigue* **119** 11–19 https://doi.org/10.1016/j.ijfatigue.2018.09.009
[11] EN 1993-1-9 2010 *Design of steel structures – Part 1.9: Fatigue* (Berlin: Beuth)
[12] ECCS Technical Committee 6 – Fatigue and Fracture 2018 *Background Documentation 9.01a – 25 Background information on fatigue design rules – Statistical evaluation – 3rd Draft (ECCS)*